Experimental Investigation of Backpulse and Backblow Cleaning of Nanofiber Filter loaded with Nano-aerosols

Curie Wing-Yee Hau and Wallace Woon-Fong Leung*

Mechanical Engineering

The Hong Kong Polytechnic University,

Hung Hom, Hong Kong

*Corresponding author

Abstract

Nanofibrous filter have been proven effective to remove nano-aerosols with particle size less than 100nm. Cleaning is required after long-term use; however, very little has been published on the subject. An experimental investigation has been launched to determine backpulse, backblow and combined backpulse-backblow on cleaning of a loaded nanofiber filter. Nylon 6 nanofiber filters were loaded with polydispersed NaCl particles, 60%<100nm and 90%<160nm, generated from an aerosol generator. Air jets in form of backpulse, backblow and their combined mode were used to clean a loaded filter. During cleaning, the filter cake was removed first for which the pressure drop across the loaded filter decreased rapidly, followed by loosely attached aerosols in the filter being removed with finite pressure drop reduction at a reasonable rate, ending in the final stage for which much lesser aerosols were being removed. Ultimately, the filter reached a residual pressure drop which was higher than that of the initial clean filter indicating residual aerosols were trapped both in the cake heel and filter.

Backpulse has been found to be more effective in removing the cake from the filter surface, whereas backblow provides an added advantage of removing

by convection of the detached aerosols away from the filter preventing recapture. The synergistic combination of backpulse-backblow provides the best cleaning performance of a nanofibrous filter loaded with nano-aerosols.

1. INTRODUCTION

Nano-aerosols are air borne (liquid/solid) particles that are about 100 nm and smaller. One source of nano-aerosols are pollutants emitted from combustion engines, in particularly diesel engines, or secondary pollutants formed from photochemical reaction of primary pollutant gases (such as NOx and reactive hydrocarbon gases) and subsequently being deposited on finer nuclei particles forming particles with size in the same range as visible light that reflect and scatter light causing photochemical smog. Another source of nano-aerosols are viruses, with sizes 10-100 nm, from common cold influenza viruses to epidemic viruses, such as middle-east respiratory syndrome virus (MERS), to bird and swine flu viruses.

Filters made from nanofibers (100-300nm) can effectively capture nano-aerosols (or referred as nano-particles with diameters < 100 nm), while conventional filters made from microfibers (1-20 μm) are less effective to capture nano-aerosols despite they can be reused after cleaning, especially for industrial applications.

Over time during filtration, the nano-aerosols (hereafter just referred as aerosols in short) deposited on the nanofibers clog up the internal pores in the nanofiber filter especially near the upstream end forming a densely populated aerosol layer, commonly referred as the skin effect that attributes to the major pressure drop of the entire filter. Subsequently, the aerosols accumulate on the filter surface eventually forming a cake. A similar phenomenon happens in the microfiber filter as well. Numerous experimental studies on pulse-jet cleaning of microfibrous filter have been carried out in the past. Previous studies [1-4] reported that the cleaning efficiency of microfiber filter is directly affected by the applied pressure of the clean air source that provides the steady jet or jet pulses. In a backpulse cleaning profile, the cleaning effectiveness is dominated by the overpressure, where the overpressure has to be sufficiently high to

overcome the adhesion force between the particles of the cake layer and the adjacent filter for detachment of the cake. Humphries and Madden[5] concluded that ineffective cleaning of pulse-bag filter is due to using an applied pressure lower than the critical value, and moderate enhancement can be made in cleaning performance by increasing slightly the applied pressure that has already reached the critical value. Other parameters, such as standoff distance between nozzle and filter, jet duration, nozzle design, nozzle diameter, etc. were also investigated [3, 6-11]. Granell and Seville[9] conducted experiments to examine the influence of standoff distance between the nozzle and the inlet of a candle filter for backpulse cleaning. They found that too short standoff distance can lead to entrainment, while too long standoff distance can result in ineffective jet pulse. Laux[3] also found that the jet duration is a trivial factor on cleaning performance, as the overpressure which dominates cleaning does not increase with the jet duration. Guidelines for testing of cleanable filter media, such as VDI 3926 [12] exist, yet they are written strictly for cleaning of loaded microfiber filters.

The technology of backpulsing on cleaning loaded filters is well-developed for microfibrous filter but it is unclear whether the same procedures can be applied to cleaning nanofiber filters as there has been virtually little-to-nil being reported in the literature. Several issues remain to be tackled for cleaning of nanofiber filters.

The first and foremost issue is that whether filter made from fragile nanofibers with diameters (100-300 nm) can be cleaned by backpulsing, backblowing, or combination to remove the filter cake deposited on the filter as well as aerosols trapped inside the filter without breaking nanofibers in the nanofibrous mat? If there is a cake already deposited on the filter, the air jet has to flow through a filter loaded with aerosols and subsequently flow through the pores of the cake. The momentum of the air jet would have been reduced by the time when it reaches the cake. Would the force be sufficiently strong to overcome the adhering force of the cake to the filter surface yet small enough not to damage the nanofibers?

The second issue is that after the cake is removed, can the jet further remove the aerosols that are trapped in the filter during depth filtration? It is expected that some of the aerosols are loosely attached to the

nanofibers and other aerosols (possibly forming dendrites) in the filter and can be removed easily, while others are strongly attached to the nanofibers by the Van der Waal force.

A third issue is whether some of the detached aerosols further get recaptured by the nanofiber filter downstream of the detachment location?

While the first three are very interesting scientific issues that pinpoint whether nanofiber filter can be cleaned, the fourth and last issue is more engineering oriented. Assuming the nanofiber can be cleaned what is the effect of applied pressure drop and pulse duration on backpulse cleaning?

The objectives of this study are centered on these four outstanding issues. The approach presented herein is largely experimental. First, we will discuss how nanofibers in the filter are prepared and characterized; this is followed by loading of the filter using polydispersed aerosols; cleaning set-up in the experiments; and results and discussions on the test results.

2. NANOFIBER FILTER

2.1 Filter Preparation

Nylon (polyamide) is selected as the material for fabricating the test nanofiber filter due to its properties which are most suitable for producing nanofibers by electrospinning. Also, filters made from nylon material have proven suitable for trapping aerosols.

Nylon 6 (N6) pellet (6mm, Aldrich) was dissolved in formic acid to produce N6 solution. Subsequently, N6 nanofibers were fabricated by electrospinning the N6 solution under an applied electrostatic field. The schematic of the needle-less electrospinning machine (NS Lab 200, Elmarco) is depicted in Figure 1. During electrospinning, high voltage is applied to the needleless rotating electrode and the collecting electrode is grounded.

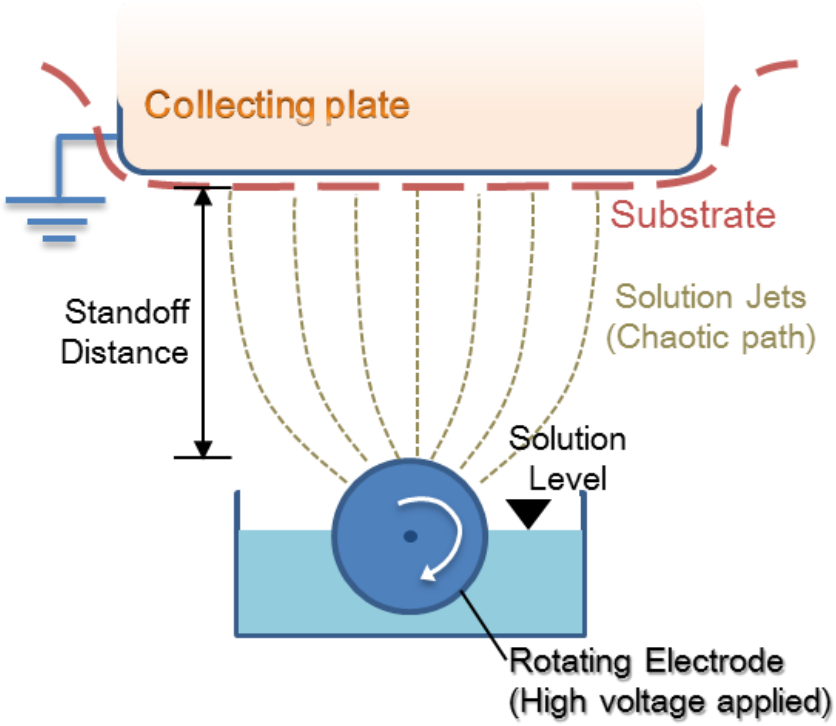

Figure 1 - Schematic of needleless electrospinning

As a departure from the traditional needle electrospinning, the rotating electrode of needle-less configuration takes form as a cylinder, or a set of wires (6 to 8), spaced circumferentially at constant radius about the axis. Upon dipping into the N6 solution, a thin film is conveyed by the rotating electrode out of the solution into the air and is exposed in a rather high-strength electric field. When the film becomes sufficiently thin, the electric force exceeds the surface tension of the thin film resulting in formation of numerous Taylor cones on the thin film surface. The Taylor cones become unstable and eventually form fibers, carrying positive charges, jetting towards the grounded collecting plate. During free flight, the positive charges deposited (from the rotating electrode) along the fiber repel each other stretching the fiber continuously. Concurrently, the formic acid solvent also evaporates under ventilation thinning continuously the fiber. Both phenomena occurring during the course of free flight result in much thinner nanofibers. The nanofibers are eventually deposited on a substrate pre-positioned on the ground collecting plate located at a standoff distance opposite to the rotating electrode. The substrate should have antistatic property to facilitate collection and the adhesion of the nanofibers to the substrate, which is important for cleaning by backblow and backpulse.

Nanofibers with mean fiber diameter ranging between 90 and 280 nm have been produced in the laboratory by adjusting the potential difference (40 – 80 kV), the standoff distance (10 – 19 cm) between the rotating electrode and the grounded collecting plate, the electrode rotating speed (6 – 50 Hz), and the concentration (14 – 22% by wt.) of the N6 precursor solution. The solidosity (solid volume fraction) and the basis weight (mass of fiber per unit filter area) can be controlled by the electrospinning time in batch production, or by the travelling speed of the substrate material during continuous production. It can also be controlled by adjusting the solution feeding rate by means of changing the electrode rotating speed.

The relationship between polymer solution concentration and the diameter of nanofibers depends mainly on the polymer used. Figure 2 shows the relationship of fiber diameter versus the solution concentration used for electrospinning. Larger fiber diameter can be obtained with more concentrated solution. As an example, to obtain fiber diameters of 200nm, the solution concentration for electrospinning should be at 18% by wt. It is worthy to note that this result also depends on the specific electrospinning setup and conditions, such as operation temperature and relative humidity. The conditions for electrospinning of nylon nanofibers are most favorable for producing 100 to 300nm nanofibers. It is known that there is an active region that a slight change in solution concentration would result in a large change in mean fiber diameter. Figure 2 further confirms this result. Indeed, as the concentration increases from 18 to 20% by wt., the fiber diameter increases exponentially. Outside this active region, increase solution concentration would only favor the formation of ribbon-shaped large “fiber diameter” which is not desirable for filtration application. On the other hand, it is more difficult to further decrease the mean fiber diameter by lowering the solution concentration alone beyond 12% by wt. An increase in applied voltage can also produce thinner diameter nanofibers.

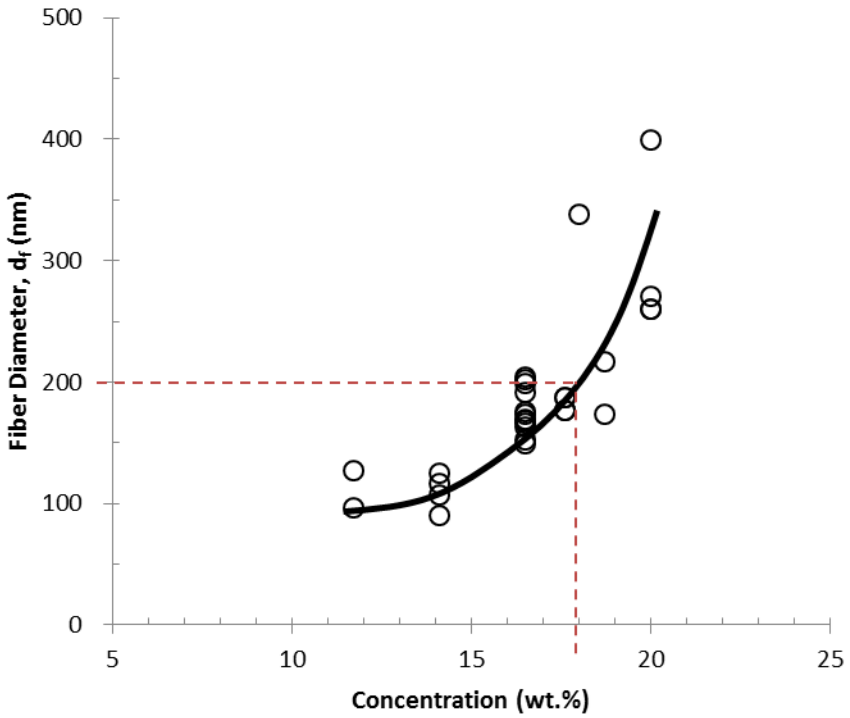

Figure 2 - Relationship of diameter of nanofibers with Nylon6 solution concentration

2.2 Filter Characterization

The images of N6 nanofibers shown in Figure 3a, b, c, respectively, for 120, 180 and 280 nm were obtained by Scanning Electron Microscope (SEM, JEOL Model JSM-6490, JEOL USA, Inc.). Not only the SEM images were used to determine the mean fiber diameters, the nanofiber shape (cross-section round or ribbon shaped) and morphology (e.g. without and with beads formation) can also be confirmed. Mean fiber diameter and fiber diameter distribution were estimated by counting at least 100 fiber diameters obtained from the SEM images by an image processing and analysis software, Image J (National Institutes of Health, US). The conditions of electrospun N6 nanofibers also depend on conductivity of the substrate material. Conventional substrate material in aerosol filtration is typically spunbond non-woven Polypropylene (PP) that has low conductivity, which hinders nanofibers production by electrospinning. Pre-treatment on the substrate is one of the several means to increase the conductivity to improve adhesion between the electrospun nanofibers and substrate. The latter is very important as it allows effective backpulse and backblow on cleaning loaded nanofiber filter without nanofibers detaching

from the substrate. By enhancing the wettability of the PP substrate by use of hydrophilic substrate, this can improve the adhesion of nanofibers onto the substrate, which is most desirable.

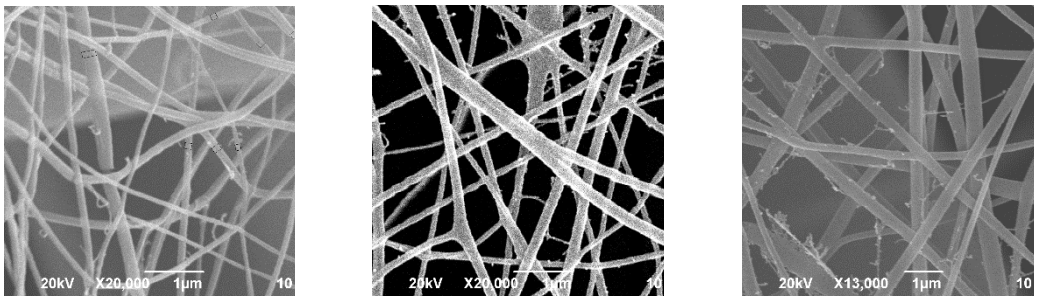

(a) (b) (c)

Figure 3 - SEM images of nanofibers with mean fiber diameter of (a)120nm, (b)180nm and (c)280nm

3. LOADING NANOFIBER FILTER

As discussed, the aerosols are distributed non-uniformly during loading of the filter with more aerosols trapped in the filter at the upstream end forming a less permeable layer in the filter – the skin layer, which accounts for the majority of the pressure drop across the filter. This increases the air flow resistance and aerosols start depositing on the surface of the filter initiating the formation of an aerosol cake. Over time, as more aerosols deposit the cake layer increases in thickness, it is possible that the cake layer is non-uniformly packed with finer aerosols infiltrating towards the bottom of the cake layer adjacent to the filter and larger aerosols deposited near the cake surface. In any event, there is flow resistance which is manifested as pressure drop across the cake as well as across the filter loaded with aerosols. The total pressure drop across the filter including the cake may have attributed largely due to the aerosol deposit in the cake especially under long-term loading resulting in a thick cake layer.

Given the pressure drop across the loaded filter also reflects largely to the amount of cake formed on the filter surface, higher pressure drop indicates a thicker cake. Thus, in the experiment the end point can be set

on aerosol loading on a filter by the pressure drop reaching an arbitrary maximum. In our experiments, it was set to about 800 Pa. Higher values are also acceptable. Alternatively, one can prescribe a fixed duration for loading the filter and the pressure drop across the filter is monitored over time up to the end of the allowed period. The maximum pressure attained at the end of fixed duration typically increases during loading as more aerosols “coat” on the surface of the filter forming a residual heel layer.

Loading a test filter using ambient air suffers from uncontrolled aerosols size, concentration distribution, and composition, all of which may also vary over time. It would be very difficult to draw comparison between different filter configurations as the feed aerosols are changing over the test period. To have a better control of aerosol loading on a filter, the N6 nanofibrous filter sample produced from electrospinning is loaded by neutralized polydispersed sodium chloride aerosol generated by a submicron aerosol generator (SMAG, model 7388L, MSP Corp., Shoreview, MN) to simulate an accelerated loading under steady-state controlled condition. The schematic layout of the SMAG for loading is depicted in Figure 4.

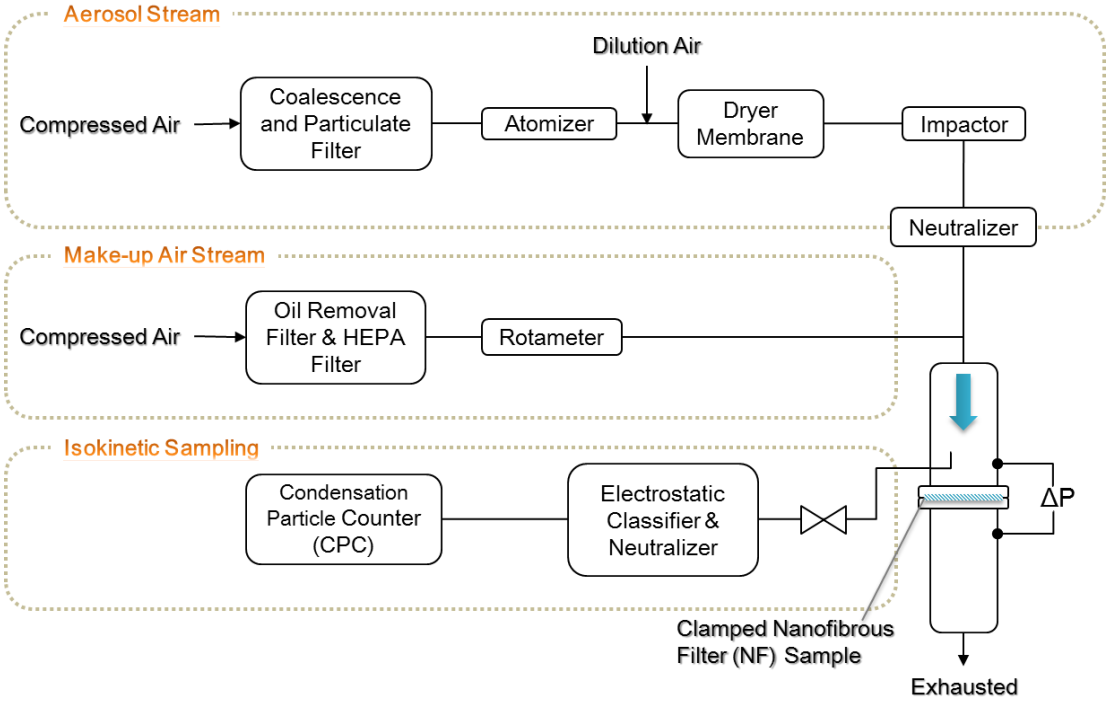

Figure 4 - Schematic of SMAG setup

Sodium chloride solid, NaCl(s), was dissolved in deionized water to form

an aqueous solution, NaCl(aq) in the atomizer. Particle size distribution varied in accordance to the concentration of NaCl(aq) being used, ranging from 0.1% to 5%. Increase in solution concentration shifted the distribution curve towards the larger particle diameter. Under continuous supply of 0.2MPa compressed air flowing into the atomizer, the NaCl(aq) was atomized into submicron particles, with sizes between 10 and 1000nm, mixed with the compressed air forming the aerosol stream. The aerosol flow rate and concentration can be varied by further mixing with dilution air. The mixed polydispersed NaCl aerosol stream was subsequently dried by passing through the air dryer made of Nafion membrane, a copolymer that enhanced moisture removal of gas stream by perevaporation. The latter was driven by water content gradient between the gas streams flowing respectively inside and outside of the membrane. The dehumidified aerosol stream then flowed through the impactor with a 90° bend so that large particles (>300nm) got captured by the impactor plate and were removed. The particle cut size depended on the impactor diameter as well as the aerosol flow rate. The remaining particles were directed to an electrical neutralizer where the high concentration air ions, generated by the electrical neutralizer, brought the incoming aerosol to conform to a Boltzmann charge distribution. The size distribution of the aerosols loading the filter is shown in Figure 5. As can be seen, large particles greater than 300nm are removed. The feed contains by count 60% less than 100nm and 90% less than 160nm. As such, it can be considered the filter is approximately loaded with primarily nano-aerosols (≤100 nm). Note that our SMAG can generate particles down to 10nm, however, the particle condensation counter cannot measure accurately the particle sizes below 50nm.

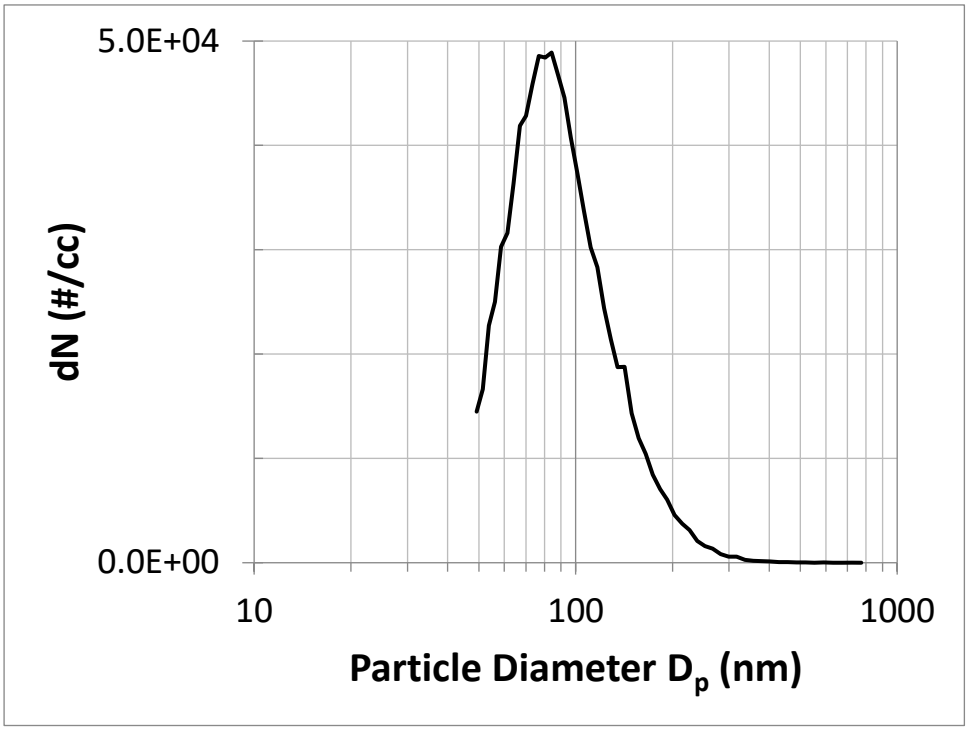

Figure 5 - Particle count concentration per cubic centimeter generated by the SMAG after large particles (>300nm) are classified.

The polydispersed aerosols stream was fed subsequently into the test column to load up the test filter mounted with the filter surface perpendicular to the incoming flow. The face velocity was controlled by mixing the aerosol stream with a dried, cleaned make-up air flow, sourced from compressed air upon removing oil using an oil removal filter and removing submicron particles using a HEPA filter. Throughout the loading process, the pressure drop across the filter was monitored by a digital pressure manometer (model 2080P, Digitron, Elektron Technology, UK) and the flow rate was measured by a flow meter (TSI-4100, TSI Incorporated,USA).....The electrospun nanofiber filter was first tested for the pressure drop and filtration efficiency at a given aerosol flow rate. First, the electrospun filter sample was being tested for pressure drop and filtration efficiency, as shown in Figure 6a. Here, the aerosol stream was first passed through the electrostatic classifier and neutralizer before sending to the test filter so that the air stream contained only monodispersed aerosols with known particle diameter. The filtration efficiency was determined by counting the particle concentration, respectively, upstream and downstream of the filter for efficiency using a condensation particle counter (CPC, model 3010, TSI Inc., Shoreview, MN).

As an example, Figure 6d shows the test efficiency of a clean nanofiber filter before loading with polydispersed aerosols.

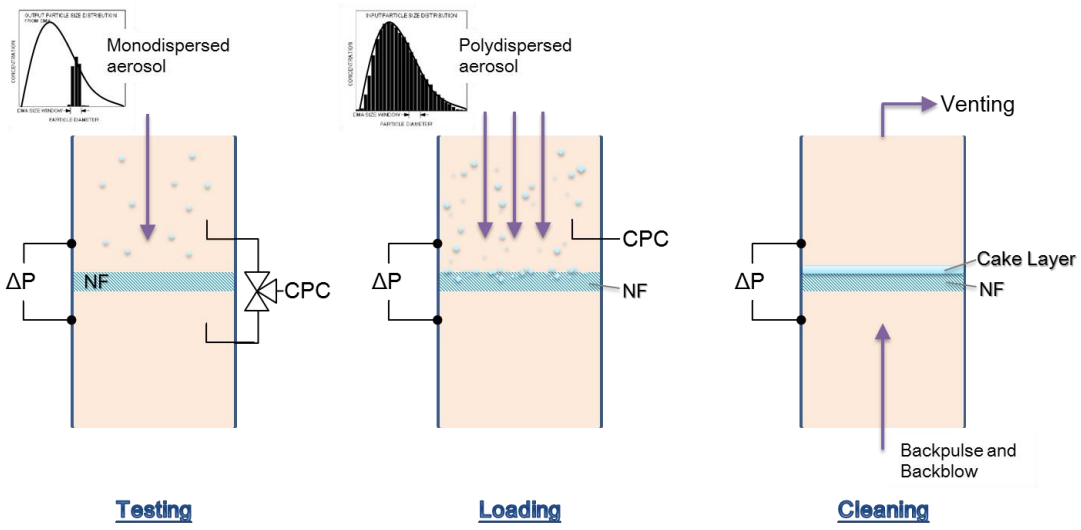

(a) (b) (c)

Figure 6 - Experiment setup of test column during consecutively (a) testing, (b) loading and (c) cleaning

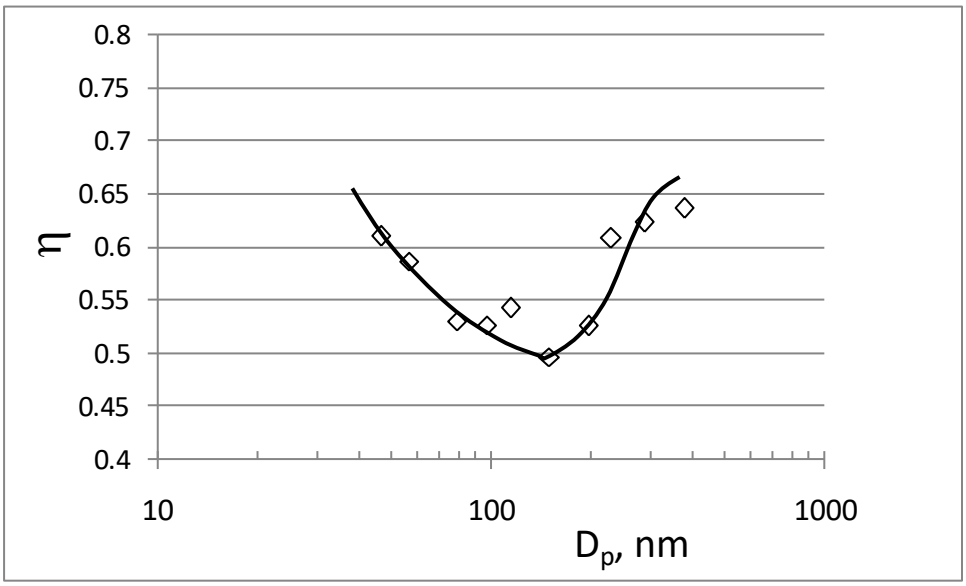

Figure 6d - Measured efficiency of a clean filter before loading with aerosols.

4. CLEANING NANOFIBER FILTER

4.1 Cleaning Setup

A three-way valve was installed before the CPC during testing to facilitate switching back-and-forth between measuring aerosol concentration in the air stream, respectively, upstream and downstream of the filter. On the other hand, as shown in Figure 6b, polydispersed aerosols were used for loading the filter and the particle size distribution was measured by upstream sampling probe connecting to the condensation particle counter. Finally, for cleaning, the setup was modified as shown in Figure 6c and the flow direction in the test column was reversed. Clean air flowed from the bottom of the test column through the filter, and the dirty air laden with aerosols removed from the loaded filter was exhausted at the top vent of the column. One regeneration methodology was composed of a series of short-duration backpulses followed by continuous airflow, or backblow. Due to the fragility of nanofibers, instead of a single air jet concentrating at one “spot”, clean air flowed through a tri-nozzle setup distributing three air jets more uniformly spreading out over a larger area against the backside of the loaded nanofibrous filter. Figure 7 shows several possible designs of tri-nozzle setup, and design (c) was finally adopted for the test setup based on simplicity in design and the superior control in delivering three uniform rate jets. Indeed, in the experiments the tri-nozzle design has proven to reduce the localized gunshot problem that has been encountered earlier by using a single nozzle for backpulse, or backblow, that broke the nanofibers found with a single-jet configuration.

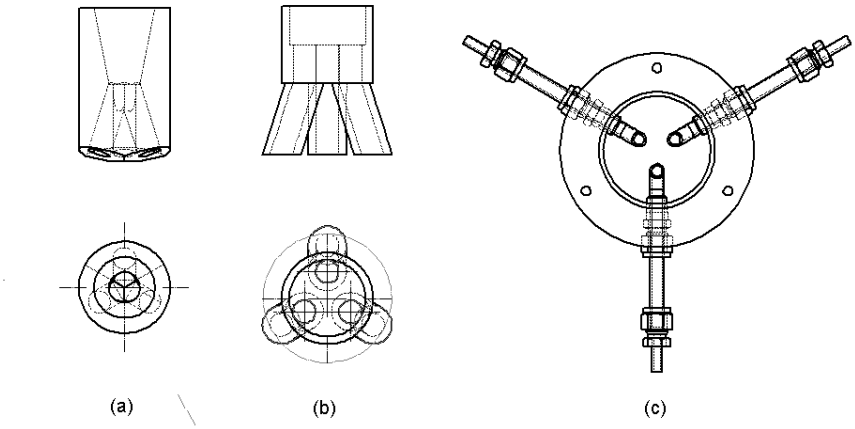

Figure 7 – Three designs of tri-nozzle setup

4.2 Backpulse and Backblow

Backpulse (BP) and backblow (BB) refer to clean air flowing from the backside or downstream side of the filter media in pulsating mode and constant-flow mode, respectively. The cleaning effect on the loaded filter media depended directly on the pressure of the compressed air source used for backpulse or backblow. From the bottom of the column, clean air flowed though a nozzle controlled by a solenoid valve to the downstream end of the loaded filter providing (a) inertial or vibration motion on the filter and cake from backpulse; or (b) shearing of trapped aerosols in the filter and cake from backblow. The settings of backpulse and backblow correspond to the opening and closing duration of the solenoid valve, respectively, which is controlled by a Programmable Logic Control with prompt and fast response based on a written “ladder diagram” that has been thoroughly tested. The nozzle was used to accelerate the flow to high velocity providing effective jet-pulses on the loaded filter.

The jet duration, idle duration, blow duration and number of pulses in a series were pre-set in the ladder diagram with counters and timers. The working logic for backpulse and backblow are depicted in Figures 8a and 8b, respectively. Note that the pressure drop shown in the figures is merely an indication of input on/off signal to the solenoid valve, thus it is written as sharp change.

The cleaning mechanism on the loaded filter from backpulse and backblow are different. Backpulse provides a finite duration air jet that impinges on the filter. The momentum of the jet is stopped by the filter translating to a series of vibration motions that loosens cake attached to the filter and the trapped aerosols in the filter. Backpulse also provides shear and drag forces on the trapped aerosols in the nanofiber filter. When these forces are sufficiently large, the cake on the filter and subsequently the trapped aerosols in the filter can be detached and removed. However, the detached aerosols (inside the filter) can be recaptured downstream of the flow.

On the other hand, backblow provides a steady continuous air stream giving rise to shear and drag forces on the cake and trapped aerosols in the filter. When these are sufficiently large overcoming the attachment forces, the cake can be blown off. Subsequently, individual aerosol as well as agglomerates of aerosols can be removed. Again, the free-flight aerosols can be recaptured

downstream of the flow by the filter. The recapture mechanism is quite complicated, as aerosols can be recaptured by the nanofibers in the filter, reattached again from the nanofibers by backpulse/backblow, and recaptured again by the filter downstream provided the filter is sufficiently long.

Backpulse and backblow can be combined to obtain synergistic effect on cleaning. Suppose backpulse is to loosen or detach the trapped aerosols via inertia excitation, backblow removes the loosened aerosols before they have a chance to become recaptured again by the filter.

The working logic of combining backpulse and backblow is depicted in Figure 8c where a series of pulse jets is executed before a constant air flow for backblow. This “cycle” is repeated during the cleaning process. Beside the opening and closing duration of solenoid valve which controls the duration of backpulse and backblow, the number of backpulses before starting backblow is also a parameter to be optimized.

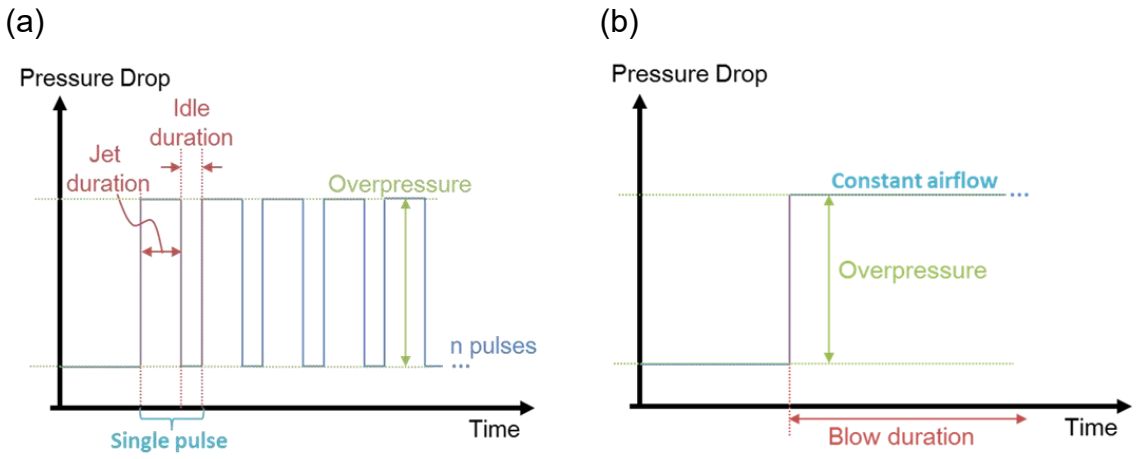

(c)

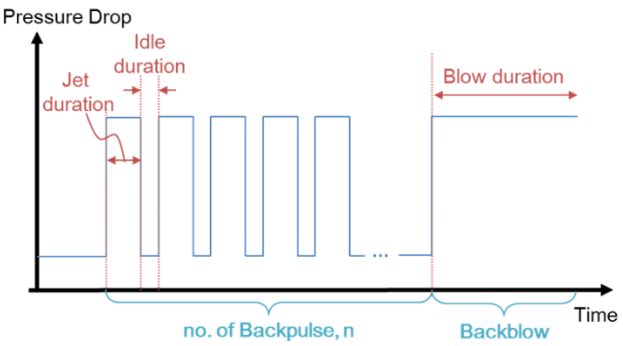

Figure 8 - The working logics of (a) backpulse, (b) backblow and (c) combined backpulse-followed-by-backblow

5. RESULTS AND DISCUSSIONS

5.1 Pressure Excursion Curve in Cleaning

Despite of variations in filter samples, loading and cleaning settings, the regeneration behavior were found to be all similar. Three characteristic stages of regeneration can be identified. First, there was a very rapid cleaning process that removed most of the deposited cake that contributed to the pressure drop in a loaded filter, thus the pressure drop decreased precipitously once the cake composed of aerosols were removed. The second stage represented a transition between the first rapid cleaning stage and the final ineffective cleaning stage. In the second stage, the remaining aerosols were more difficult to be removed and this involved aerosols migration dislodging from one location and reattaching possibly to the filter further downstream of the flow. This seemed to be a time-dependent slow process, and the pressure drop decreased slowly over time. In the third and final stage, the pressure drop remained nearly constant despite continuous backpulse or backblow. This indicated that little-to-nil additional trapped aerosols were removed and the "residual pressure drop", Δp_r, reflected the residual aerosols remaining in the filter.

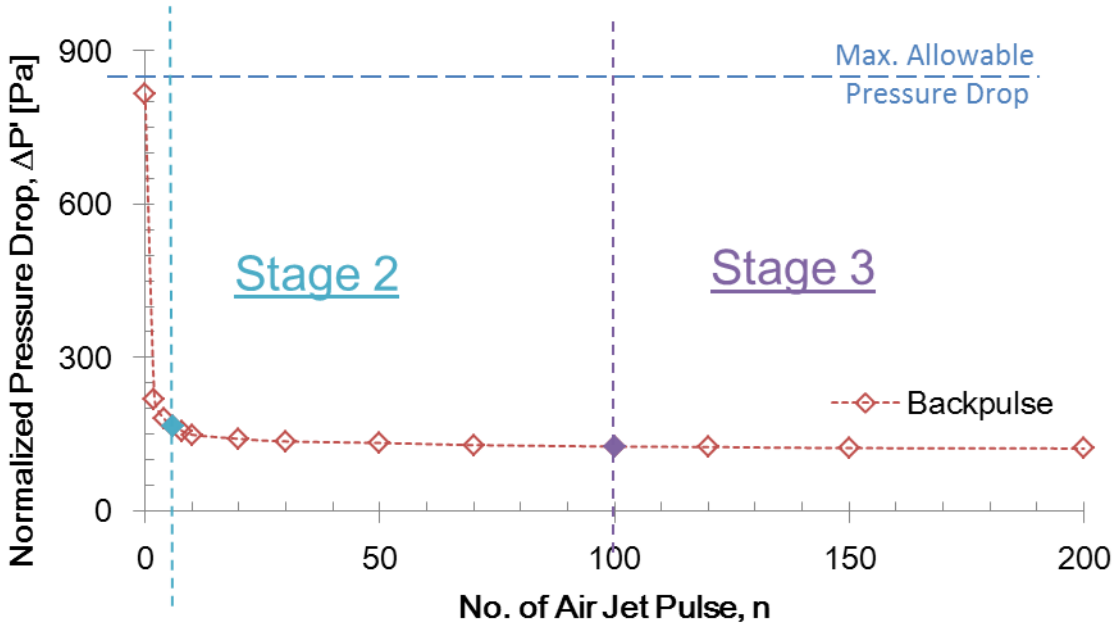

Figure 9 - Example of three cleaning stages for nanofibrous filters

Figure 9 shows an example on the cleaning behaviour. (Note that the tank pressure for the air jet was set to 6.5 bars for all the experiments with the exception for the experiments where the pressure of the tank was deliberately varied to explore the effect of the tank pressure on cleaning a loaded filter.) The filter was loaded with aerosols under steady condition to the maximum pressure drop of 840Pa. Once the pressure drop reached this maximum level, loading was halted and filter cleaning was ensued subsequently. The results of backpulse cleaning on a test filter sample is shown in Figure 9, where the normalized pressure drop, $\Delta P'$, is the pressure drop of a loaded filter, ΔP, with reference to the clean filter pressure drop, ΔP_f, i.e. $\Delta P' = \Delta P - \Delta P_f$.

The demarcation of the three stages for backpulse is as follows:

Stage 1: $$\left|\frac{d\,(\Delta P')}{dn}\right| \geq 30 \qquad \text{----------(1)}$$

Stage 2: $$0.1 < \left|\frac{d\,(\Delta P')}{dn}\right| < 30 \qquad \text{----------(2)}$$

Stage 3: $$\left|\frac{d\,(\Delta P')}{dn}\right| \leq 0.1$$ ----------(3)

Where $\Delta P'$ is the normalized pressure drop

n is the number of jet pulses.

The values of 30 and 0.1 are quite arbitrary. For backblow, the three stages are defined as follows:

Stage 1: $$\left|\frac{d\,(\Delta P')}{dt}\right| \geq 30$$ ----------(4)

Stage 2: $$0.1 < \left|\frac{d\,(\Delta P')}{dt}\right| < 30$$ ----------(5)

Stage 3: $$\left|\frac{d\,(\Delta P')}{dt}\right| \leq 0.1$$ ----------(6)

where dt is the backblow duration.

Before discussing the results, it is useful to quantify the cleaning using a residual ratio. Residual ratio is a convenient indirect measure of the percentage of aerosols staying in the filter after cleaning using recorded pressure drop across the filters at various conditions. It is defined as the ratio of the residual pressure drop Δp_r minus the clean filter Δp_f, to the maximum loaded filter pressure drop Δp_o minus the clean filter Δp_f, as given by Eq. 7.

$$\text{Residual ratio} = \frac{\Delta P_r - \Delta P_f}{\Delta P_o - \Delta P_f} = \frac{\Delta P'_r}{\Delta P'_o}$$ ----------(7)

Where ΔP_f is the clean filter pressure drop of filter,

ΔP_o is the maximum pressure drop on loaded filter before

cleaning,

ΔP_r is the pressure drop of filter after cleaning,

$\Delta P'$ is the normalized pressure drop.

5.2 Backpulse and Backblow in Nanofibrous Filters

To investigate the effect of backpulse and backblow in cleaning loaded nanofibrous filter, two experiments were carried out separately. In both cases, the filter was loaded under the same condition. In one case, the loaded filter was cleaned by backpulse alone. In another case, the loaded filter was cleaned by backblow alone. In both cases, the maximum allowable pressure drop was arbitrary set at 840 Pa. The mean fiber diameter of the two filter samples used in the two tests was 180 nm with the clean filter pressure drop measured to be 30 Pa at a face velocity of 5.3 cm/s.

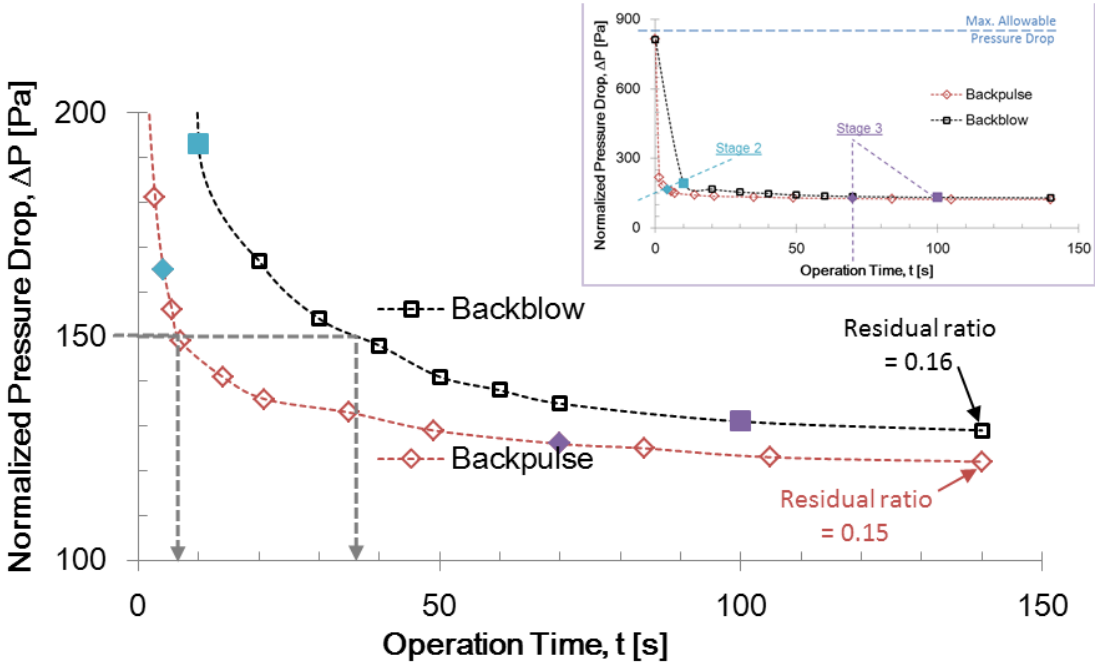

Figure 10 - Cleaning curves of two preloaded nanofibrous filters cleaned, respectively, by backpulse alone and by backblow alone.

To compare the effectiveness of the two approaches, the cleaning curves are

plotted with pressure drop against operation time in Figure 10. For backpulse, each single pulse with duration of 0.7s consisted of 0.5s jet pulse and 0.2s of idle. For backblow, a time interval based on 10s was set to ensure that the duration for valve in opening position was sufficiently long to develop steady flow for which a steady air jet could be realized in the test. For both experiments, after 138s (2.3 min) of cleaning the residual ratio was determined to be 0.16 for backblow alone and 0.15 for backpulse alone. While the end points reached by the two methods were not too far different, the time to attain an intermediate pressure drop was much faster for backpulse than with backblow. By means of an example, to achieve the pressure drop of 150 Pa, the time needed for backpulse was 6s which was about 1/6 that required for backblow cleaning, namely 36s. This reveals that backpulse is a more efficient cleaning process. Therefore, in terms of effectiveness or efficiency, backpulse is a better choice than backblow in filter regeneration. This is due to the inertia force or shock that backpulse exerted on the loaded filter loosening the cake and removing the cake by the flow. It took about 4s (end of first stage) for the cake to be removed by backpulse, see also inset figure in Figure 10, and the pressure drop was at 165Pa. Once the cake was removed, the trapped aerosols in the filter could be removed by further backpulsing by first detaching the aerosols from anchoring to the nanofibers and subsequently carrying these loosened aerosols in the flow away from the filter.

With backblow, the shear force has proven to be less effective in dislodging the cake from the filter. It took almost 10s to dislodge the cake and some aerosols still remained trapped on the filter surface in a thin residual cake layer (referred hereafter as the “cake heel”) as the pressure drop was at 193Pa, which was much higher than 165Pa as seen with backpulse at the end of first stage. Additional backblow was required to remove the cake heel before cleaning off the aerosols trapped by nanofibers in the filter. In fact, 10s additional time was required to clear the cake heel to attain the same pressure drop condition as with backpulse, both at 165Pa, see Figure 10.

In the experiments discussed in the foregoing, the cleaning effectiveness of backpulse and backblow were compared revealing backpulse being better than backblow. This is especially in removing the cake from the nanofiber filter. However, the synergy of the combined mode may be advantageous as the two mechanisms each works best under certain conditions. Instead of using backpulse to carry the loosen aerosols away from the nanofiber filter, it may be

advantageous in providing a steady flow to carry the detached aerosols from residing in the nanofiber filter for which they can be easily recaptured. To that end, further experiments were carried out to investigate the cleaning behaviour of loaded filter first by backpulse to be followed by backblow, and the result is compared with that of cleaning by backpulse alone in Figure 11. In the experiment, there were 10 pulses in a series of backpulses (i.e. n=10), for which each single pulse consisted of 0.5s jet pulse followed by 0.2s of idle. After the 10 backpulses, it was followed by 10s of backblow. This “cleaning cycle” was repeated. The backpulse setting for the backpulse only was the same as with the backpulse in the combined mode.

In terms of efficiency, cleaning by backpulse alone is better initially as the time spent in cleaning is minimized, see Figure 11. This is especially in the cake removal stage (first stage) where faster pressure drop occurs with consecutive backpulses providing a series of consecutive shocks to the filter and cake, rather than consecutive combined backpulse followed by backblow as the subsequent backblow in the combined mode did not help to speed-up the cake removal, instead, it took slightly longer time.

On the other hand, the result shows that the combined backpulse and backblow (combined regeneration) have better cleaning effectiveness in the second and third stages with ultimate lower residual pressure. In fact, the pressure drop in the second stage is faster for the combined mode than just the backpulse mode alone. It can also be seen in Figure 11 that the slope of a secant line drawn between the two points on the backpulse curve at 100^{th} pulse and 200^{th} pulse (at transition from second to third stage) is less for the backpulse as compared to that for the combined mode. This is because with additional backblow followed by backpulse, the detached aerosols got carried further downstream, if not out, of the filter with reduced chance of being recaptured by the nanofiber filter. This mechanism of efficient removal of detached aerosols in the nanofiber filter extended from the second to the third stage with the combined mode having a steeper decrease in pressure drop as compared with the backpulse alone. Indeed, the ultimate residual ratio at the end of the third stage dropped down to 0.13 for the combined regeneration, which is lower than 0.15 for backpulse cleaning alone. It can be seen in this comparison that backpulse alone is most effective for cake removal at the early stage, in the second and third stages additional backblow can effectively remove the aerosols reducing the chance for recapture of detached aerosols.

It is to be noted that despite backpulse is best for the cake removal in the first stage, whereas backpulse-followed-by-backblow is best for second and third stages for purging aerosols in the filter once the cake has been blown off. To avoid using sophisticated monitoring and control switching from backpulse in the first stage to backpulse-backblow in the second and third stages, it is more practical to use backpulse-backblow in the entire regeneration starting from the first stage all the way to the third stage.

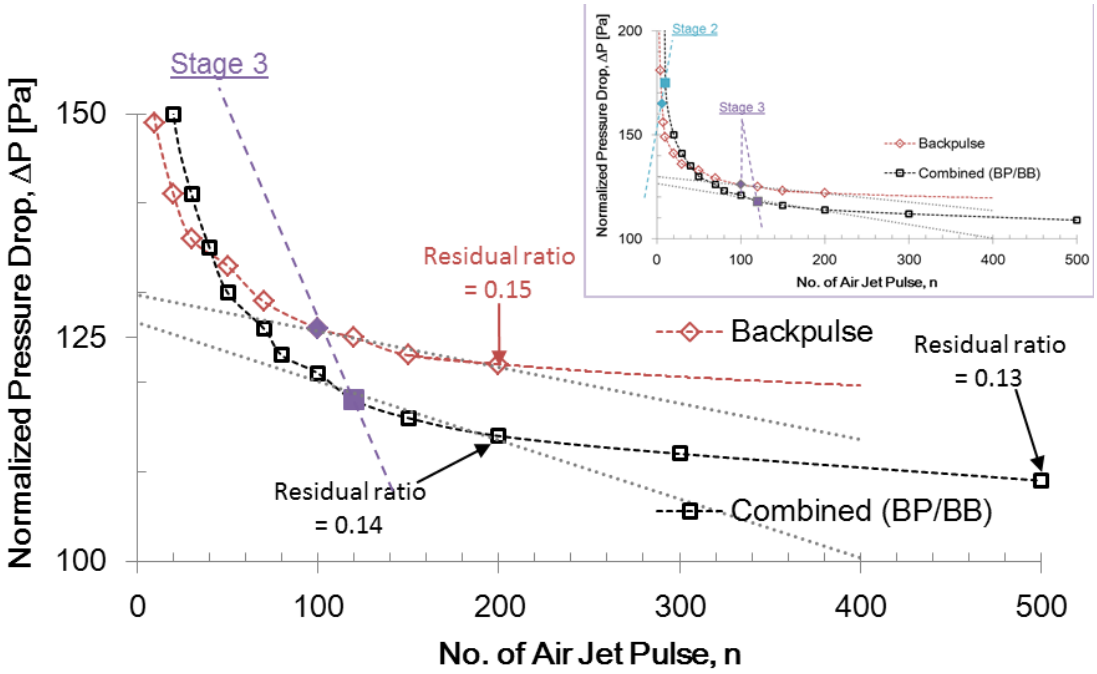

Figure 11 - Comparing cleaning curves of nanofibrous filter cleaned with backpulse alone with backpulse-followed-by-backblow.

5.3 Jet Duration

It was suggested [3] that a sudden change of over-pressure on the downstream end of the filter is the unique factor for backpulse cleaning and jet duration is not responsible for cleaning a conventional baghouse dust collector. This might not work for the nanofiber filter. To tackle this issue, the jet duration effect on backpulsing a loaded nanofiber filter was investigated.

All the cleaning conditions were kept constant with the exception of the backpulse jet and idle durations. There were three sets of backpulse settings

representing three different valve response times for drawing comparison. They were considered as fast, moderate and slow responses corresponding to 0.1s, 0.3s and 0.5s respectively. To modify the variations, the idle duration was set to be identical as the jet duration. For example, for moderate valve opening time, both jet duration and idle duration were set at 0.3s.

The results are shown in Figure 12. There were two sets of experiments, one set in which cleaning was a combined backpulse followed by backblow, whereas the other set corresponds to backpulse alone. Both experiments were stopped at 300th pulse (i.e. n=300) and the final pressure drop across the filter was taken as the residual pressure drop. As with the previous case, cleaning with combined backpulse-and-backblow resulted in lower residual ratio, as depicted in this Figure 12, due to effective blowing-away of the detached aerosols. More importantly, increasing from 0.1 to 0.5s jet duration resulted in lower residual ratio. Both sets indicate that longer jet duration is beneficial to lowering the residual pressure drop, thus lowering residual aerosols in the filter. Longer jet duration produces a larger air volume with high momentum that resulted more intense vibration and shock on the filter that can loosen the trapped aerosols in the filter. Hence, the jet duration indeed makes a difference to cleaning unlike conventional baghouse filter.

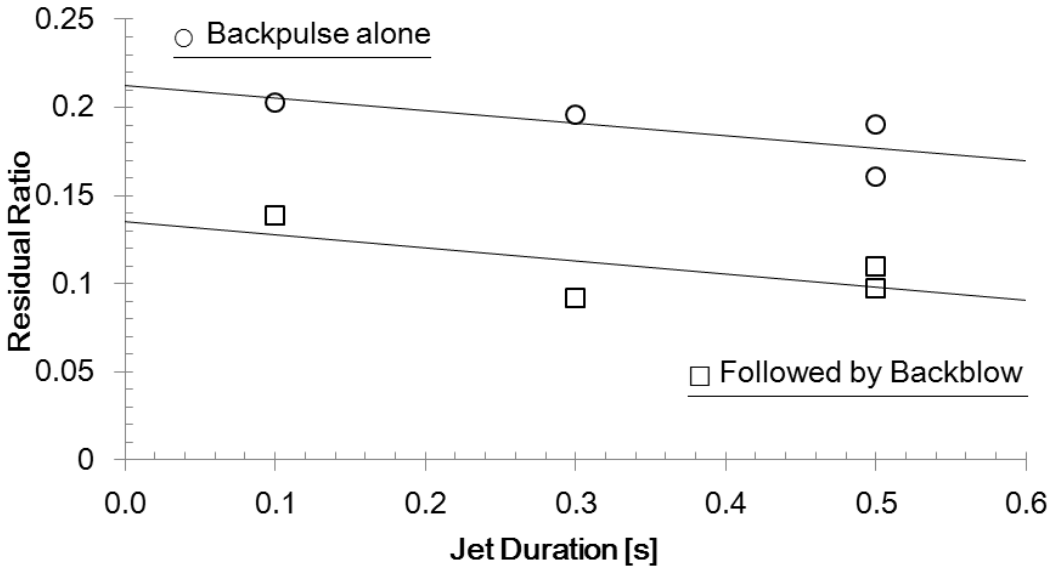

Figure 12 - Residual ratios of nanofibrous filters cleaned by different jet duration

5.4 Applied Pressure

The effect of applied pressure on nanofibrous filter cleaning was investigated experimentally. The loading and cleaning conditions were remained unchanged across the experiments. The only variation was the compressed air tank pressure which considered as low, moderate and high applied pressure, i.e. 3 bar, 4 bar and 6.5 bar respectively. The results are plotted in Figure 13. The residual ratio of for the filter cleaned with low applied pressure, 3 bar, doubles that of high applied pressure; while the case with moderate applied pressure is in between the two. This shows that the cleaning efficiency increases with the magnitude of applied pressure, similar to the case of conventional microfibrous filter cleaning. However, it is worth noting that there is an upper limit of applied pressure due to the fragility of nanofibers which depends on the fiber diameter, fiber mat thickness, adhesion between nanofibers and its supportive substrate, the cleaning setup configurations (i.e. standoff distance of jet, single versus multiple jets, jet velocity, area coverage and uniformity of jet impingement). The three jets from the tri-nozzle setup have been able to reduce jet impingement from a single vigorous jet focusing on a concentrated area on the filter, which otherwise can induce local damage on the nanofiber filter.

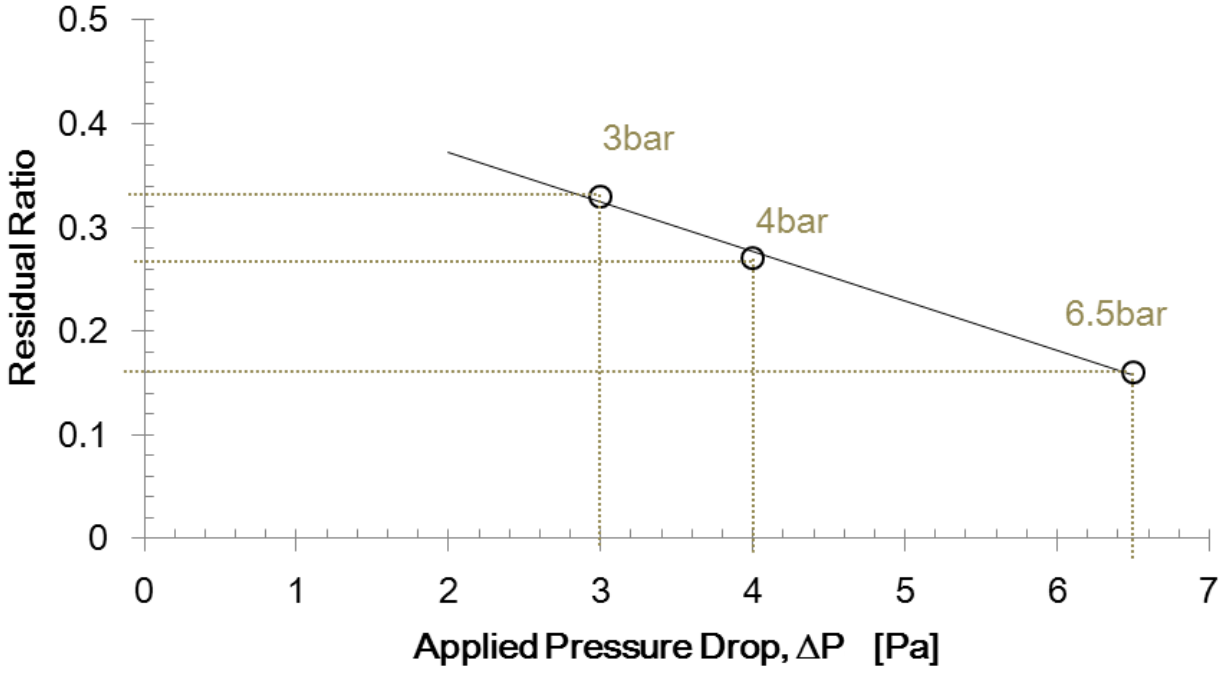

Figure 13 - Residual ratios of nanofibrous filters cleaned by different applied tank pressure

6. CONCLUSIONS

Cleaning can be effectively carried out by backpulse, backblow and a combined backpulse-followed-by-backblow to remove nano-aerosols trapped in the filter by depth filtration and in the cake by surface filtration.

Three stages for cleaning are typically observed - a first stage where cake is removed for which pressure drop across the loaded filter reduces significantly and rapidly over time, a second stage for which lesser aerosols are removed for which loosely attached aerosols trapped inside the filter are detached and removed, and a third stage where the mechanisms are similar but much less aerosols are removed as the aerosols are more firmly adhered to the nanofibers. Loosened aerosols can possibly be recaptured downstream of the flow for both second and third stages. The pressure drop reduction from cleaning is progressively less in the second stage and more so in the third stage. The pressure drop ultimately reaches an equilibrium residual level.

Backpulse cleaning is to provide inertial force in form of a shock to the loaded filter and pulsating jet pulse of air to remove the loosened aerosols. Backblow cleaning is to provide shear to overcome the attachment of aerosols to the nanofibers, and also air flow to remove loosened aerosols. Backpulse is found to be more effective for cleaning than backblow in all three stages. However, it is best to use the inertial force of backpulse to loosen the cake from the filter, as well as the aerosols inside the filter from the nanofiber attachment; and use the convection from the backblow to remove loosen aerosols from the filter preventing recapture. This synergistic effect has been demonstrated to be better than backpulse alone, which pertains especially for the second and third stages in removing aerosols inside the filter.

Three key parameters play an important role in use of air stream to clean loaded filter. Higher pressure in the pressurized source provides more favorable conditions for cleaning for backpulse, backblow and their combination. The advantages have been demonstrated for test pressures in the pressurized source at 3, 4, and 6.5 bars respectively. The impingement of the jet on the backside of the loaded filter needs to be distributed uniformly about the filter to avoid single shot-gun effect that can break the nanofiber mat. A tri-nozzle spray has been found to be more favorable to deliver a uniform area of cleaning than

a single jet. Furthermore, for backpulse it has been found that longer pulse duration of 0.5s is better than shorter pulse duration to provide a stronger inertial force on cleaning the loaded filter.

7. ACKNOWLEDGEMENTS

The authors thank The Hong Kong Research Grant Council for supporting the project and supporting Curie WY Hau for two years of her studentship under Project B-Q33G. The authors also thank Hung-Faat Choy for his help during the course of experiments.

REFERENCES

[1] M. De Ravin, W. Humphries, R. Postle, "A model for the performance of a pulse jet filter," *Filtration and Separation*, vol. 25, no. 3, pp. 201-207, 1988.

[2] J. Sievert, F. Löffler, "Fabric cleaning in pulse-jet filters," *Chemical Engineering and Processing: Process Intensification*, vol. 26, no. 2, p. 179–183, 1989.

[3] S. LAUX, U. RENZ, "Pressure cleaning of ceramic filter elements for the hot gas filtration," *Dissertation RWTH Aachen*, 1993.

[4] R. Mai, M. Fronhöfer, H. Leibold, "Flow characteristics of filter candles during recleaning," *High Temperature Gas Cleaning*, pp. 194-206, 1996.

[5] W. Humphries, J.J. Madden, "Fabric filtration for coal-fired boilers: dust dislodgement in pulse jet filters," *Filtration and Separation*, vol. 20,

no. 1, pp. 40-44, 1983.

[6] H.C. Lu, C.J. Tsai, "Numerical and experimental study of cleaning process of a pulse-jet fabric filtration system," *Environmental science & technology*, vol. 30, no. 11, pp. 3243-3249, 1996.

[7] H.C. Lu, C.J. Tsai, "A pilot-scale study of the design and operation parameters of a pulse-jet baghouse," *Aerosol science and technology*, vol. 29, no. 6, pp. 510-524, 1998.

[8] H.C. Lu, C.J. Tsai, "Influence of design and operation parameters on bag-cleaning performance of pulse-jet baghouse," *Journal of Environmental Engineering*, vol. 125, no. 6, pp. 583-591, 1999.

[9] S.K. Grannell, J.P.K. Seville, "Effect of venture inserts on pulse cleaning of rigid ceramic filters," *High Temperature Gas Cleaning*, vol. 2, pp. 96-110, 1999.

[10] J.H. Choi, Y.G. Seo, J.W. Chung, "Experimental study on the nozzle effect of the pulse cleaning for the ceramic filter candle," *Powder Technology*, vol. 114, no. 1-3, pp. 129-135, 2001.

[11] L.M. Lo, D.R. Chen, D.Y.H. Pui, "Experimental study of pleated fabric cartridges in a pulse-jet cleaned dust collector," *Powder Technology*, vol. 197, no. 3, pp. 141-149, 2010.

[12] P. Geang, Update of VDI-Guideleine 3926 "Testing of Filter Media for Cleanable Filters" and Development of a Mobile Filter Probe for Field Measurements", 6th Symposium "Textile Filters", March 5th and 6th 2002, Chemnitz, Germany.